

Supplemental Materials

Molecular Biology of the Cell

Borinskaya et al.

Figure S1. CD16/7-mCherry-VCA and CD16/7 (Empty) fusion protein expression and co-expression in NIH-3T3 transfected cells.

A Western blot demonstrating expression (anti-CD16) of CD16/7-mCherry-VCA (black arrow) and CD16/7 (empty arrow): 100% VCA, 100% Empty, 60% VCA with 40% Empty, 37% VCA with 63% Empty, 15% VCA with 85% Empty. A double band is observed for each CD16/7 fusion protein: the top band is the full-length fusion protein; the bottom band is a cleaved fusion protein lacking the aggregatable CD16 domain.

Figure S2. VCA turnover via SynZip binding interface in membrane clusters.

A. (Left) Fluorescent recovery after photobleaching (FRAP) of mCherry-VCA in CD16/7-eYFP-SynZip1 : SynZip2-mCherry-VCA clusters as compared to (Right) FRAP of mCherry-VCA in CD16/7-mCherry-VCA clusters. x-axis: time, seconds. y-axis: average integrated intensity of N-WASP or VCA cluster, normalized.

B. Western Blot of CD16/7-eYFP-SynZip1 (detected with anti-GFP antibody) and SynZip2-mCherry-VCA (detected with anti-dsRed antibody) expression in NIH3T3 cells. Lane (1) - wild type cells; lane (2) - cells expressing CD16/7-eYFP-SynZip1; lane (3) - cells expressing SynZip2-mCherry-VCA; lane (4) - cells co-expressing CD16/7-eYFP-SynZip1 and SynZip2-mCherry-VCA. Positions of molecular weight markers (MWM) are indicated to left.

C. Recruitment and clustering of SynZip2-mCherry-VCA after antibody-mediated aggregation of CD16/7-eYFP-SynZip1 (*top panel*). Without aggregating CD16/7-eYFP-SynZip1, SynZip2-mCherry-VCA does not cluster (*bottom panel*). Scale bars=10 μ m.

Figure S3. Nck SH3(1-2-3) recruits the adaptor protein Dip by GST pull-down assay.

293T cells were transfected with plasmids expressing YFP-DIP or mVen-mDia1. Whole cell lysates (WCL) of transfected cells were incubated with either GST or GST-Nck SH3(1-2-3) purified proteins immobilized on GSH beads. WCL or elution fractions from the beads were immunoblotted with anti-GFP antibody to detect YFP-DIP and mVen-mDia1 and with anti-GST antibody to detect GST and GST-Nck SH3(1-2-3) proteins bound to the GSH beads.

Figure S4. Formin FH2 domain inhibition disrupts comet tail shape of Vaccinia-induced actin structures.

A. Vaccinia-induced actin comets in fixed HeLa cells. Staining: actin (Phalloidin /red), Vaccinia (immunostaining, CFP/shown in green). *Top panel*: control cell (DMSO). *Bottom panel*: cell treated with the 100 μ M formin inhibitor SMIFH2.

B. Morphology analysis of Vaccinia-induced actin aggregates in DMSO-treated (control) and in SMIFH2-treated fixed HeLa cells. (*DMSO-treated*: 3 cells, 282 aggregates; *SMIFH2-treated*: 4 cells, 136 aggregates). Error bars are mean \pm s.e.m. **P*<0.005.

Figure S5. Formin FH1 domain overexpression for inhibition of endogenous formin activity at membrane clusters (Fig. 5).

A Western blot demonstrating overexpression of mVenus tagged FH1 domain (anti-GFP) as compared to endogenous level of FH1 domain. *WT*: not transfected NIH-3T3 cells.

Ctrl: cells transfected with CD16/7-mCherry-Nck SH3 and mTFP1-actin. *Ven-mDia1*: cells transfected with CD16/7-mCherry-Nck SH3, mTFP1-actin and mVenus tagged full-length mDia1 (detected with anti-GFP and anti-mDia1). *Ven-FH1* (5 lanes): cells transfected with CD16/7-mCherry-Nck SH3, mTFP1-actin and mVenus tagged FH1 domain (detected with anti-GFP); *Ven-FH1* cell lysate was diluted 1/25, 1/50, 1/100, 1/200, 1/400 times. Loading control: cortactin.

Figure S6. Comparison of actin structures induced by membrane clustering of Nck SH3 and N-WASP VCA with EPEC actin pedestals.

A. Schematic of signaling cascade to branched actin nucleation in cells infected with *Vaccinia* virus. Not shown in the schematic is that N-WASP recruitment requires WIP, and that A36 also recruits Grb2, which enhances comet tail formation.

B. *Vaccinia*-induced actin comets in HeLa cells. Staining: actin (pseudo colored green/Phalloidin), *Vaccinia* (pseudo colored red/vB5R-GFP virus).

C. Schematic of signaling cascade to branched actin nucleation in cells infected with EPEC bacteria.

D. Infection of 3T3 cells with EPEC results in formation of actin pedestals. Staining: actin is stained with phalloidin 488 (green) and EPEC is labeled with mouse anti-LPS and alexa 568 anti-mouse secondary (red). Scale bars=5 μ m.

E. Morphology comparison of Nck- and VCA-induced actin structures, *Vaccinia* actin comet tails and EPEC actin pedestals. (*Nck*: 3 cells, 540 aggregates; *VCA*: 3 cells, 336 aggregates; *Vaccinia*: 9 cells, 371 aggregates; *EPEC*: 16 cells, 477 aggregates). Error bars are mean \pm s.e.m. * $P < 0.01$, ** $P < 0.001$.

F. Velocity comparison of Nck- and VCA-induced actin structures, *Vaccinia* actin comet tails and EPEC actin pedestals. (*Nck*: 7 cells, 654 aggregates; *VCA*: 7 cells, 945 aggregates; *Vaccinia*: 7 cells, 125 aggregates; *EPEC*: 13 cells, 405 aggregates.)

Figure S1

CD16/7-mCherry-VCA	1.00	0.00	0.60	0.37	0.15
CD16/7 (Empty)	0.00	1.00	0.40	0.63	0.85

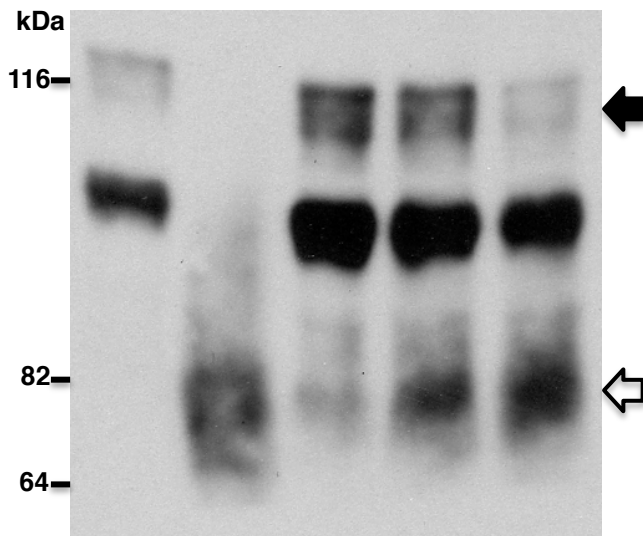


Figure S2

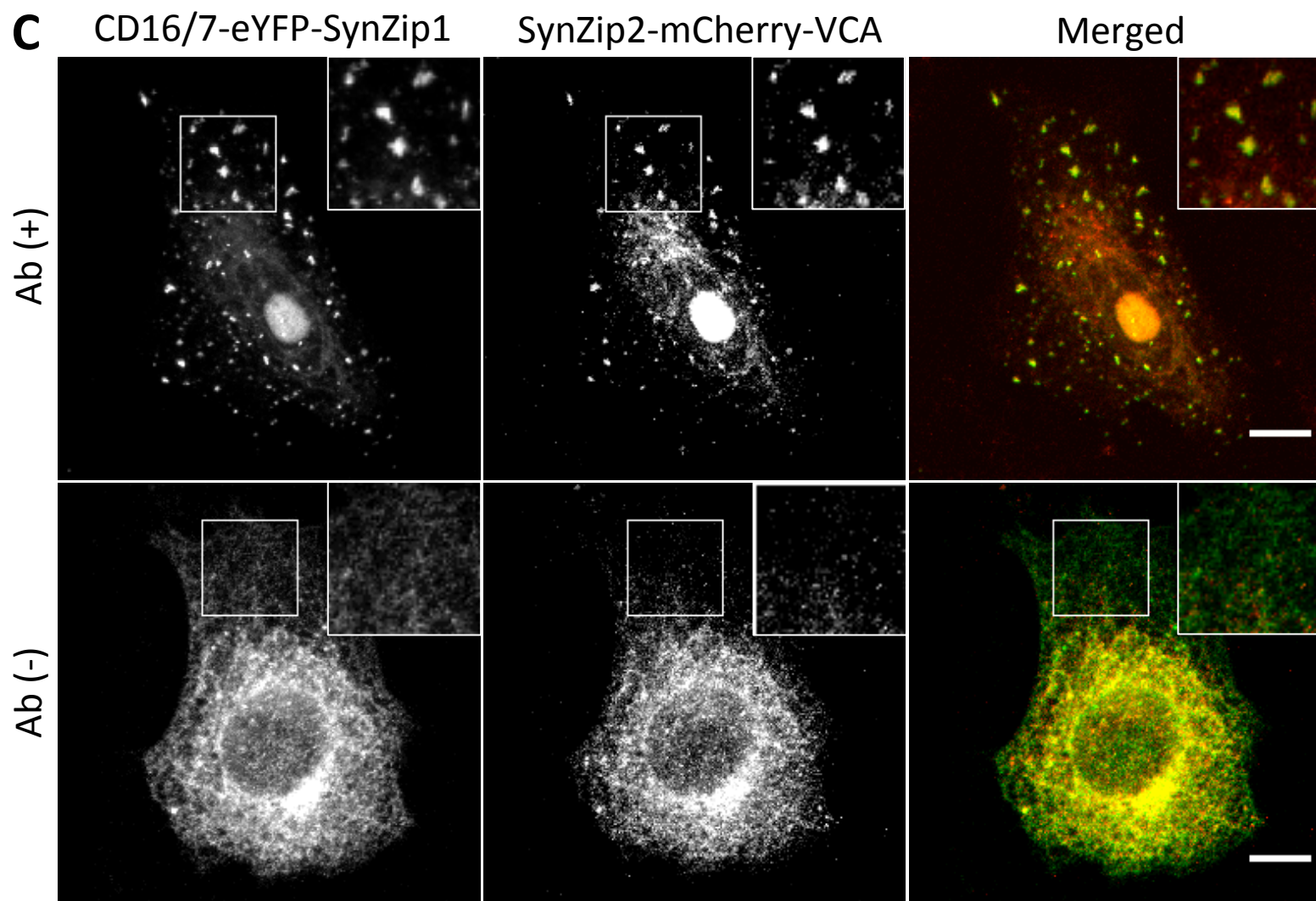
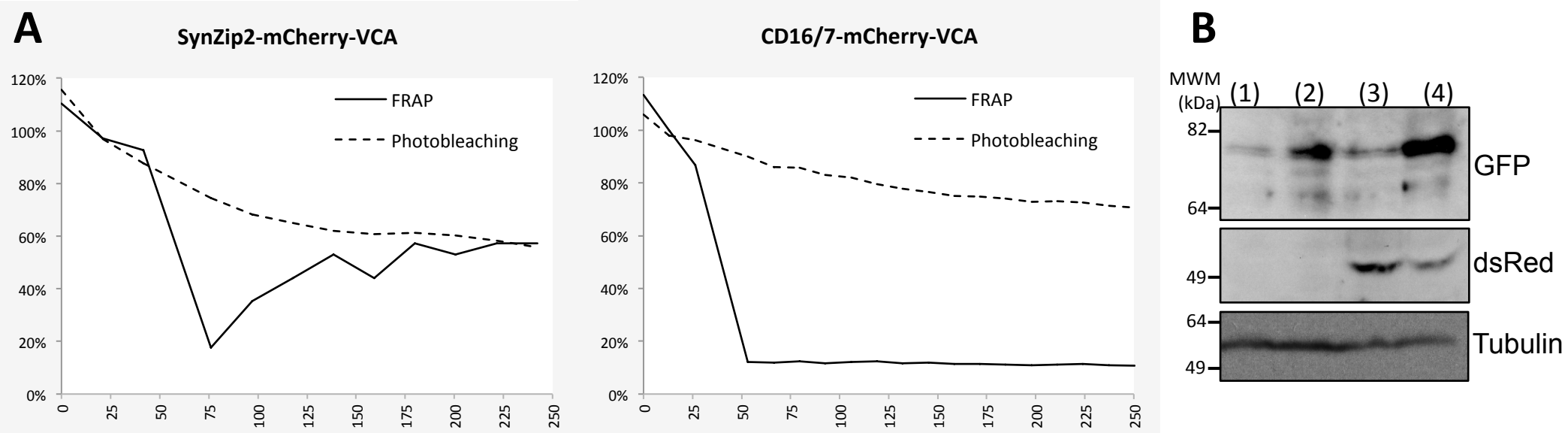


Figure S3

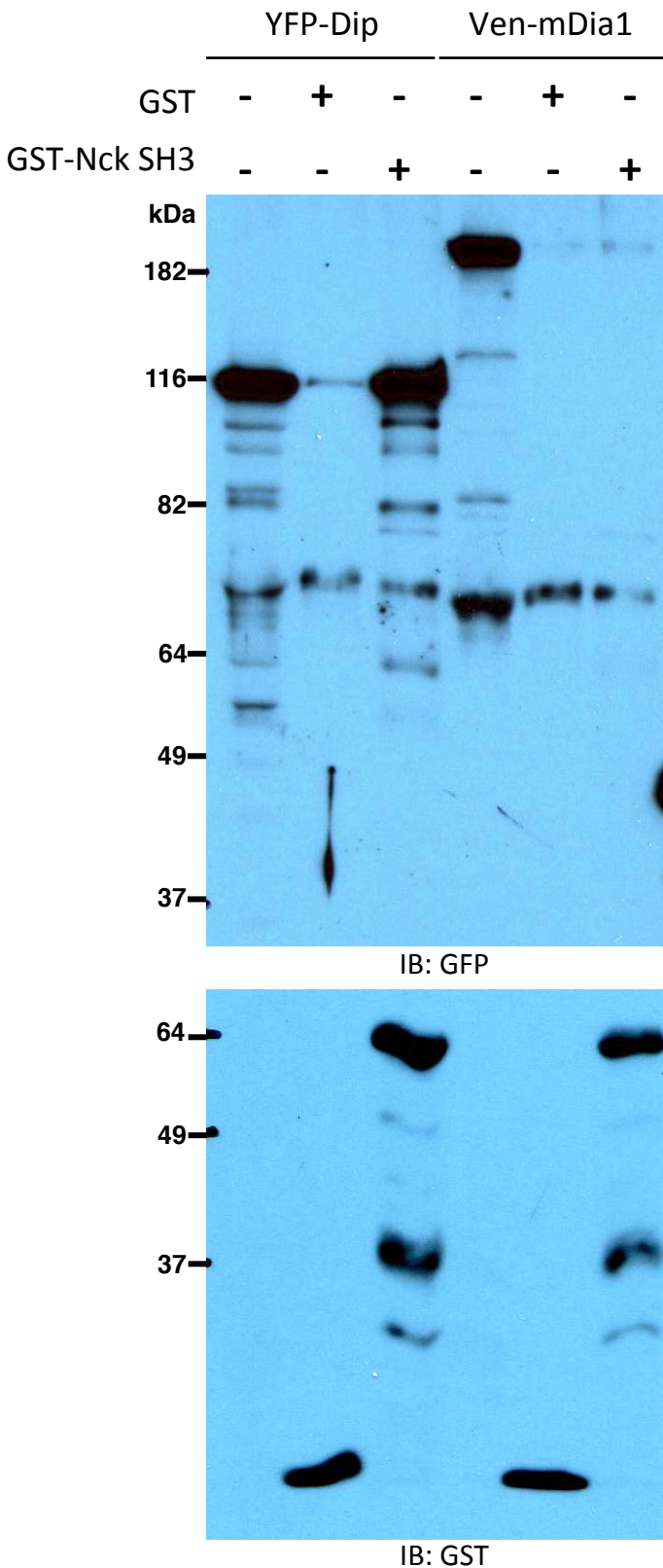


Figure S4

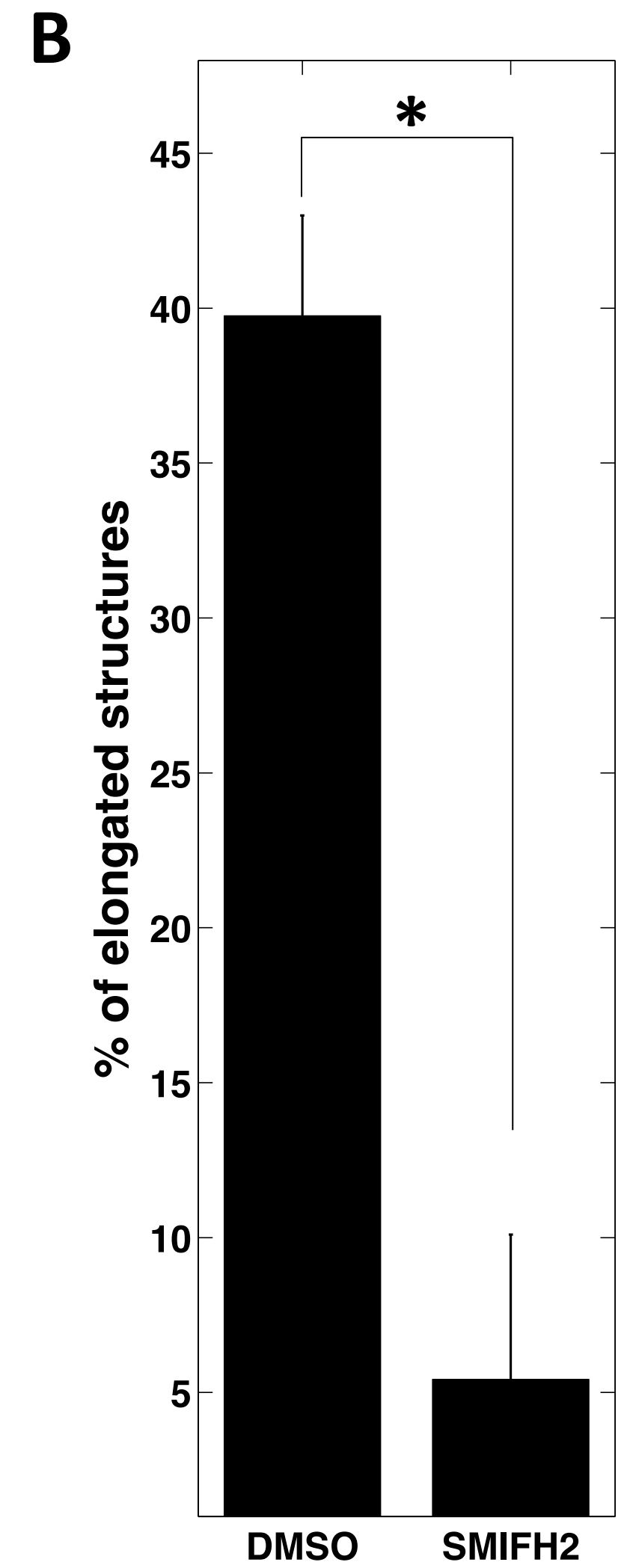
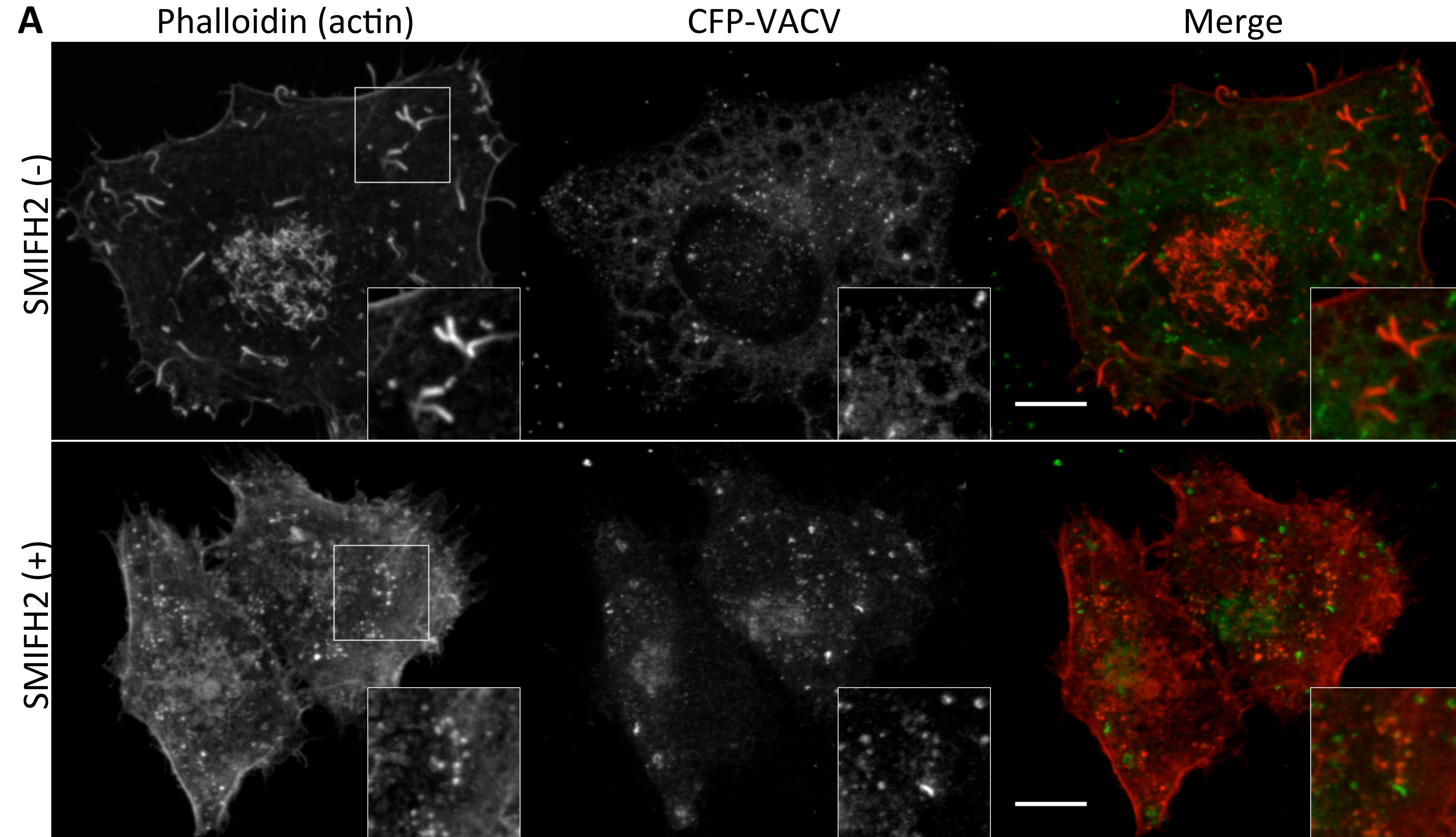
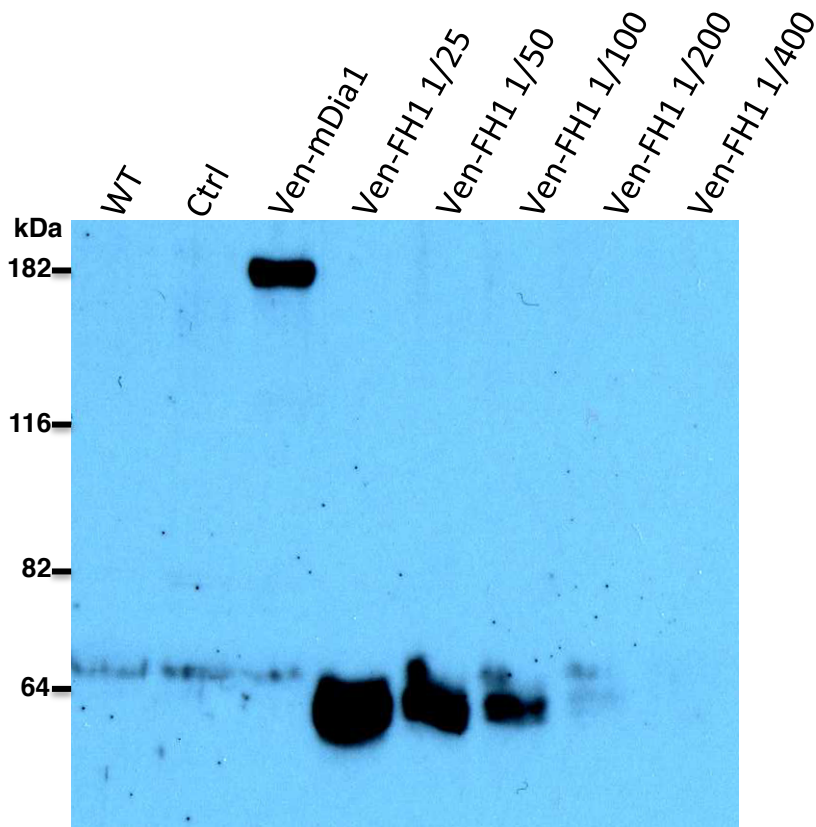
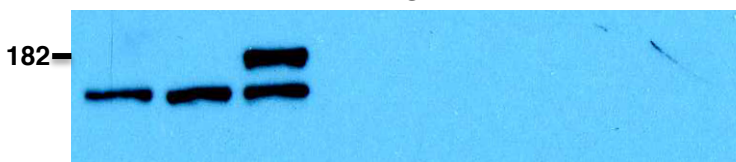


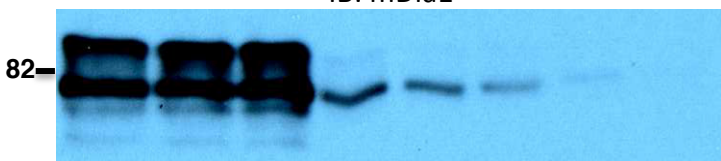
Figure S5



IB: GFP



IB: mDia1



IB: Cortactin

Figure S6

